Influence of stress state based on hydraulic-mechanical coupling and water loading path on fault activity

Yujie Zhu
Key Laboratory of Geotechnical Mechanics and Engineering of Ministry of Water, Changjiang River Scientific Research Institute Wuhan, China
Tsinghua University, Beijing, China

Chen Xu (corresponding author)
Changjiang Institute of Survey Planning Design and Research, Wuhan, China
Tsinghua University, Beijing, China

Yingguo Hu
Key Laboratory of Geotechnical Mechanics and Engineering of Ministry of Water, Changjiang River Scientific Research Institute Wuhan, China

Xiaoli Liu, Enzhi Wang
Tsinghua University, Beijing, China

ABSTRACT: In the exploitation of shale gas and enhanced geothermal energy, reservoir water storage and carbon dioxide storage projects, induced earthquakes are closely related to the activity of primary faults. A fractured cylinder sample with 60° inclination is adopted in the indoor test. The shearing test is used to explore the impact of different stress critical conditions and pore water pressure loading paths on the triggering mechanism and mechanical behavior of fault activity, providing reference for the reservoir impounding plan. The test shows that when the increased pore water pressure is the same, the higher the critical pressure, the greater the displacement of fault sliding and the more energy released. Pore pressure under different path loading has influence on the process of fault dislocation, but has less effect on the displacement of the fault. The stress state and pore water pressure determine the fault displacement.

Keywords: Stress state, HM coupling, loading path, induced seismicity.

1 INTRODUCTION

The shear release energy of the primary fracture under the combined action of the stress field and the seepage field forms the induced earthquake, which is a problem faced by many projects such as shale gas exploitation, enhanced geothermal development (Zang et al. 2014), reservoir water storage, carbon dioxide storage, etc., and poses a threat to the safety of the project and personnel. At present, through laboratory tests, numerical simulation and field tests, the cognition of the dislocation of the seepage field change of cracks or faults under the action of high ground stress has gradually deepened, but its failure mechanism still needs to be further discussed.

In practical engineering, cyclic load (including cyclic stress load and seepage stress load) has become an important factor affecting the failure of rock and soil mass. Therefore, the laboratory test can fully simulate the stress cyclic loading path in nature and study its failure mechanism. Under natural conditions, the rock and soil gradually fatigue under the influence of cyclic pulse load, resulting in the failure of its mechanical strength and the destruction of the structure (Zuzulock et al. 2020). The study on weakening of rock tensile strength during dry-wet cycle shows that after repeated cycles of dry-wet, the tensile strength and stiffness of rock are reduced and the ductility is enhanced.

Its degree is not only related to the number of cycles, but also closely related to the content of clay minerals in the sample (Guo et al. 2021). The tensile failure caused by cyclic hydraulic fracturing of granite core shows that compared with the fractures produced by continuous injection of rock, cyclic hydraulic fracturing can produce more complex fractures with more branches and smaller pore sizes. Circulating water injection can reduce the breakdown pressure by 20% and the maximum acoustic emission amplitude by 14%. It shows that in the process of hydraulic fracturing, alternating injection of fluids with high flow rate or high water pressure can reduce seismic activity (Zhuang et al. 2019). Triaxial tests of quartz-rich sandstone show that cyclic injection may cause less seismic activity than monotonic injection, providing a new insight into the fluid-solid interaction affected by changes in circulating fluid pressure (Noël et al. 2019a, 2019b).

2 EXPERIMENT METHOD

2.1 Sample preparation and test equipment

Granite is used which is mainly composed by feldspar, quartz, biotite and hornblende. Its density is 2610kg/m^3, uniaxial compressive strength reaches 186MPa, rock modulus is 84GPa, and Poisson's ratio is 0.25 (Zhu et al. 2020). The granite is processed into a cylinder with a diameter of 50mm and a height of 100mm, and it is symmetrically cut into two parts with two 2mm diameter holes. The inclination of the cut surface is 60° from the horizontal bottom of the cylinder. We polish the crack surface with P600 abrasive paper to make the surface smooth and reduce the roughness. The sample is assembled by a teflon thermoplastic sleeve. Figure 1 shows schematic of the set up.

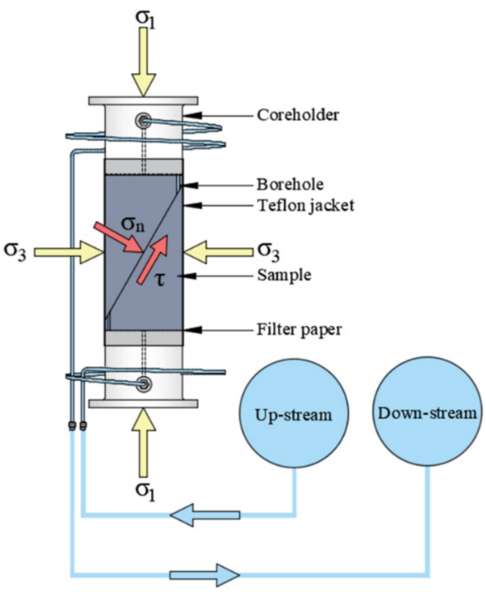

Figure 1. Schematic diagram of triaxial test setup.

2.2 Test steps and analysis methods

All the shear flow experiments are conducted under constant normal stress with certain water pressure. The variation of water pressure is described in two types (Figure 2): one is increasing water pressure from 5 MPa directly to 8 MPa at the rate of 0.005 MPa/s, defined as monotonic injection strategy (MI); another is increasing water pressure from 5 MPa to 6 MPa, 7 MPa and finally 8 MPa periodically, simulating cyclic injection strategy (CI). Based on the impounding strategy, we design four tests as shown in table 1. The RI-1 and RI-2 tests adopts cyclic injection strategy. The RI-3 and RI-4 tests adopts monotonic impoundment strategy.

Table 1. Boundary conditions of tests.

Sample	Impoundment strategy	Confining pressure (MPa)	r_τ
RI-1	CI	13	98%
RI-2	CI	14	93%
RI-3	MI	13	95%
RI-4	MI	14	93%

In the MP test, the upstream water pressure increased to 8MPa at the rate of 0.005MPa/s after 600s, and maintained for 1000s so that the water can be fully and evenly distributed on the fault surface and finally reach the equilibrium state. The water pressure at the downstream outlet is measured and counted to monitor the fracture sliding rule.

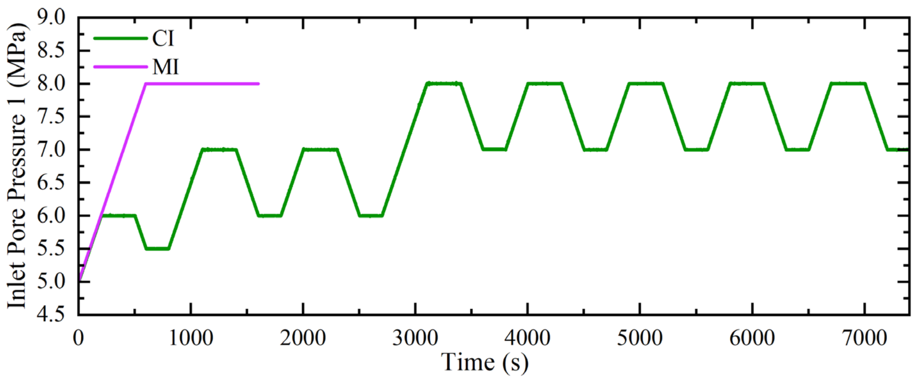

Figure 2. The water loading path of monotonic impoundment (MI) and cyclic impoundment (CI).

The process of CP test is that the water pressure in the fracture increases in a periodic and stepwise manner. As shown in Figure 2, each cycle has four steps: water level rises to high water level, maintains high water level, water level falls to low water level, and maintains low water level. Based on the injection with constant pressure rate, the test consists of three stages. In the first stage, the water level rises from 5MPa to 6MPa at 0.005MPa/s within 200s, and remains for 300s, then drops to 5.5MPa, and remains for 200s. The second stage includes two cycles. The water pressure rises to 7MPa from the end of the last cycle, lasting for 300s, and then drops to 6MPa and lasting for 200s. The third stage includes five cycles, with the maximum water pressure of 8MPa for 300s and the low water pressure of 7MPa for 200s.

3 RESULTS

3.1 Fracture sliding characteristics of cyclic injection strategy

The RI-1 test and RI-2 test show the cyclic injection strategy. The results show that under the periodical water pressurization, the fault slip happens periodically. Figure 3 and Figure 4 shows the shear displacement and output pore pressure in the four tests.

The RI-1 fault becomes unstable when the inlet pressure linearly increases from 5 to 6 MPa. The friction coefficient is 0.87 and the ratio r_τ between shear stress and shear strength is 98%. There are 23 slip events in the 8 cycle. The fault failure is expected when the water pressure exceeds 5.2 MPa. The fault begins to slip in the first cycle when the output pressure reaches 5.30MPa. In the second cycle, the occurrence of the slip events is accompanied by the slight drop in outlet pressure and the remarkable increase until the outlet pore pressure reaches 5.5 MPa. Slip events disappear when the outlet pressure reaches 7.87 MPa. The maximum slip distance is 54.12μm and the accumulate slip distance is 1.63mm. The maximum slip rate is 1.74mm/s.

The RI-2 is stable when the inlet pressure oscillates from 5 to 8 MPa. The ratio r_τ is 93%. The theoretical failure pore pressure is 6.4 MPa. There are 7 events in this test. The outlet pore pressure increases in a nonlinear rate. The first slip event happens in fourth cycle when the highest pore pressure reaches 8 MPa. The last slip occurs in the seventh cycle. The total shear displacement of the fault is 0.415mm. This distance is much less than the value in RI-1 test. The maximum slip rate is 1.62mm/s.

3.2 Fracture sliding characteristics of monotonic pressurization

The RI-3 test and RI-4 test show the monotonic injection strategy. The results show that the fault consistently slides after the pore pressure increases and seismic becomes aseismic after the outlet pore pressure keep constant. (Figure 3 and Figure 4)

In RI-3 test, the theoretical failure pore pressure is 5.9 MPa. The ratio r_τ is 95%, a little less than the ratio in RI-1. There are 25 seismic events in the test, which has two more events than RI-1. The fault begins to slip when the outlet pore pressure exceeds the theoretical value. Besides, the slip distance tends to smaller after 25 seismic events. The fault becomes aseismic when the outlet pore pressure keeps constant. The maximum slip rate is 0.41mm/s. The accumulative shear displacement is 1.17mm. This data is also a little less than that in RI-1.

In RI-4 test, the theoretical failure water pressure is calculated to be 6.2 MPa. The phenomenon is similar to RI-3. But the seismic events are 8 in this test. The fault slides consistently with the pore pressure increase. Still the slip distance tends to decrease after several slip. The accumulative shear displacement is 0.425mm, which is quiet similar to the value in RI-3. The maximum slip distance is 59.4 μm and the maximum slip rate is 2.01 mm/s.

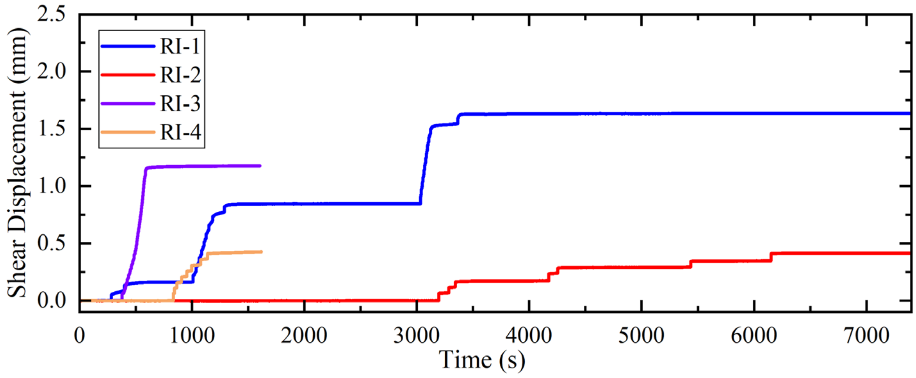

Figure 3. Shear displacement of induced seismicity in laboratory test.

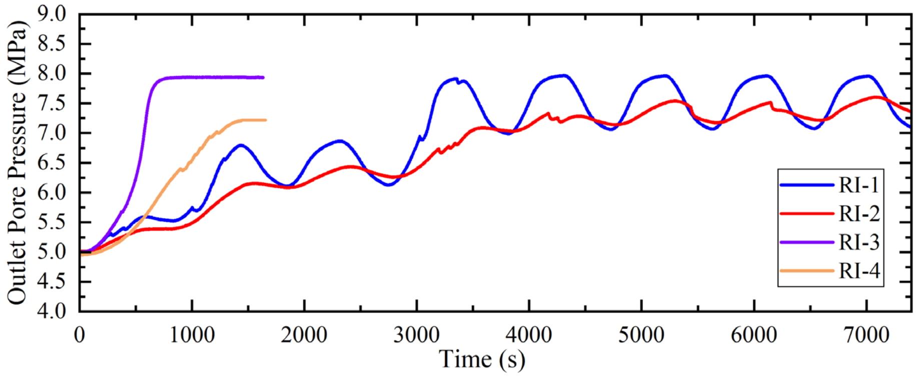

Figure 4. Outlet pore pressure of induced seismicity in laboratory test.

4 DISCUSS

4.1 Hydraulic energy

Hydraulic energy is introduced in this research to illustrate the influence of stress state and water loading path on induced seismicity. Hydraulic energy (E_H) is defined as the product of injection rate (*Q* m3/s) and injected fluid volume (*P* Pa/s) (Goodfellow et al. 2015). According to the conservation of energy, the input energy equals to the output energy. Therefore, the input energy including injection energy, which is the hydraulic energy in this test and potential elastic energy ΔW. The output energy includes frictional energy E_f (Kanamori & Brodsky 2004), radiated energy E_r(Boroumand & Eaton 2012), deformation energy E_d and energy loss *l*. The calculation of these parameters are showing in the following.

$$E_H = \int_{t_1}^{t_2} PQdt \tag{1}$$

$$\log_{10}(E_R) = 1.5M_w + 4.8 \tag{2}$$

$$E_H + \Delta W = E_f + E_R + E_d + l \tag{3}$$

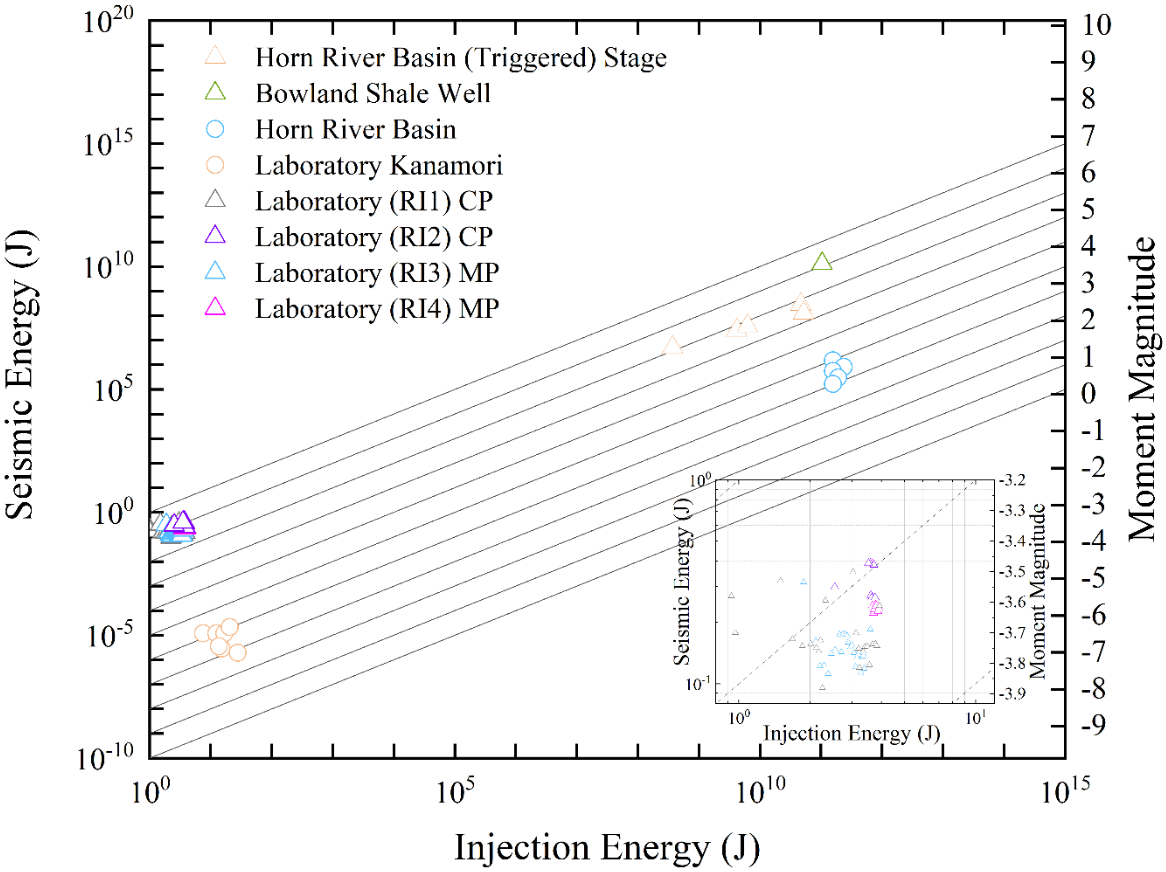

Figure 5. Injection energy plotted against seismic energy and moment magnitude.

According to the formulation, the radiated energy is referring to the seismic energy. Therefore, we use seismic energy to represent seismic energy in this article (Figure 5). The result shows that although the seismic events happens more frequently under much critical stress state, the average moment magnitude is smaller than that in lower stress state. Apartment from this, the moment magnitude of monotonic injection strategy is easier to predict than the cyclic injection strategy.

5 CONCLUSION

Fault reactivation under unconventional extraction is a threaten in construction safety. Fault in different stress state and different injection strategy would behave differently. To illustrate how the stress state and water pressure loading path influence the fault activity, we conduct four tests using fractured samples with 60° inclination to demonstrate the influence of stress state and water pressure loading path on fault induced seismicity. Monotonic injection tests and cyclic injection tests are designed to simulate different loading path of the fault. The alteration ration of shear stress and critical shear stress indicates the different stress state of a fault. Results show that the state stress can significantly effects the mechanic behavior of the fault. The closer to the critical stress state, the much easier does unstable slides happen for a fault. Which means the slip will occur at a lower water pressure with more seismic events. Furthermore, the relationship between output seismic energy and input hydraulic energy indicates that the fault will release more energy in more critical stress state under the same hydraulic condition, no matter how the pore pressure increases. Otherwise, different loading path of water pressurization can change the mechanical characteristic of fault motivation, slightly affecting the total energy release under the same stress state.

ACKNOWLEDGEMENTS

This research was funded by the Open Research Fund Program of State key Laboratory of Hydroscience and Engineering (sklhse-2022-D-01, sklhse-2022-C-04), Hubei Provincial Natural Science Foundation of China (2022CFB673).

REFERENCES

Boroumand, N., & Eaton, D. W. 2012. Comparing energy calculations: Hydraulic fracturing and microseismic monitoring. *In 74th EAGE Conference and Exhibition incorporating EUROPEC*, *European Association of Geoscientists & Engineers*, cp-293 Copenhagen, Denmark.

Goodfellow, S. D., Nasseri, M. H. B., Maxwell, S. C. & Young, R. P. 2015. Hydraulic fracture energy budget: Insights from the laboratory. *Geophysical Research Letters* 42(9), pp: 3179-3187. DOI: 10.1002/2015gl063093

Guo, P., Gu, J., Su, Y., Wang, J. & Ding, Z. 2021. Effect of cyclic wetting–drying on tensile mechanical behavior and microstructure of clay-bearing sandstone. *International Journal of Coal Science and Technology*, pp: 1-13. DOI: 10.1007/s40789-020-00403-3

Noël, C., Passelègue, F. X., Giorgetti, C. & Violay, M. 2019a. Fault reactivation during fluid pressure oscillations: Transition from stable to unstable slip. *Journal of Geophysical Research: Solid Earth*, 124(11). DOI: 10.1029/2019jb018517

Noël, C., Pimienta, L. & Violay, M. 2019b. Time-dependent deformations of sandstone during pore fluid pressure oscillations: Implications for natural and induced seismicity. *Journal of Geophysical Research: Solid Earth* 124(1), pp: 801-821. DOI: 10.1029/2018jb016546

Zang, A., Oye, V., Jousset, P., DeichmaSnn, N., Gritto, R., McGarr, A., Majer, E. & Bruhn, D. 2014. Analysis of induced seismicity in geothermal reservoirs - An overview. *Geothermics* 52, pp: 6-21. DOI: 10.1016/j.geothermics.2014.06.005

Zhu, Y., Liu, X., Enzhi Wang. 2020. Influence of impoundment gravity and pore pressure on reactivation of faults[J]. *Geomechanics and Geophysics for Geo-Energy and Geo-Resources* 6(4), pp: 1-19.

Zhuang. L., Kim, K. Y., Jung, S. G., Diaz, M., Min, K.-B. & Zang, A. 2019. Cyclic hydraulic fracturing of pocheon granite cores and its impact on breakdown pressure, acoustic emission amplitudes and injectivity. *International Journal of Rock Mechanics and Mining Sciences* 122. DOI: 10.1016/j.ijrmms.2019.104065

Zuzulock M. L., Taylor O-D. S.. & Maerz N. H. 2020. Soil fatigue from induced seismicity. *Advances in Civil Engineering* 2020, pp: 1-9. DOI: 10.1155/2020/7030425

Kanamori, H., & Brodsky, E. E. 2004. The physics of earthquakes. *Reports on Progress in Physics* 67(8), pp: 1429-1496. DOI:10.1088/0034-4885/67/8/r03